**SAHC2014** – 9th International Conference on
Structural Analysis of Historical Constructions
F. Peña & M. Chávez (eds.)
Mexico City, Mexico, 14–17 October 2014

# LIMIT ANALYSIS IN LARGE DISPLACEMENTS OF MASONRY ARCHES SUBJECTED TO VERTICAL AND HORIZONTAL LOADS

**N. Cavalagli, V. Gusella and L. Severini**

Department of Civil and Environmental Engineering, University of Perugia, via G. Duranti, 93, 06125, Perugia, Italy
{nicola.cavalagli, vittorio.gusella}@unipg.it, lauraseverini@strutture.unipg.it

**Keywords:** masonry arch, large displacements, limit analysis, horizontal loads

**Abstract.** *This work aims to analyze the behavior of masonry arches at collapse. The study fits into the frame of limit analysis referring to Heyman's theory. The collapse mechanism is of rotational type, since it shows the relative rotation of the masonry voussoirs around the so-called hinges, which occur at the edge of the thickness. In particular, two types of arches are analyzed, the circular and pointed one. The loading system consists in vertical and horizontal loads, which refer respectively to the self-weight and to the seismic actions. In a first step the collapse mechanism, the corresponding horizontal load multiplier and the horizontal thrusts at abutments are determined, in the condition of rigid abutments, as functions of geometrical features of the structure. Moreover, the minimum thickness of the arch is determined as function of the horizontal load multiplier. Finally, the circular arch with elastic abutments is studied. The failure conditions are determined as functions of the flexibilities at the abutments. The minimum thickness that the circular arch should have to stand is determined as function of the horizontal load multiplier and the flexibilities at the abutments.*

# 1 INTRODUCTION

The masonry arch has been widely studied during the last decades, especially to improve the understanding of historical constructions, for their conservation and restoration.

The turning point in studies on the stability of masonry buildings occurred in the early sixties, when Jacques Heyman extended the limit analysis, initially developed for steel structures, to the so-called *Stone Skeleton*. The application of the classical approach of limit analysis to the masonry arch [1] requires the definition of *i)* equilibrium condition, *ii)* resistance criterion, *iii)* mechanism condition. The first *i)* and the second *ii)* correspond respectively to the individuation of a thrust line in equilibrium with external loads and anywhere contained in the boundary of the arch. The third condition *iii)* corresponds to a rotational mechanism, with hinges that grow at the edge of the thickness, if the following hypothesis about the masonry are assumed [2]: masonry has no tensile strength, the compressive strength of masonry is infinite, sliding failure does not occur.

The stability of masonry arches is considered as a geometric problem, namely a right shape design is needed to achieve a safe state. Heyman [1] gives the law of the minimum thickness for the circular arch subjected just to self-weight, as function of the angle of embrace. The analysis on the minimum thickness in the presence of the self-weight has been recently extended also to pointed arches [3].

The influence of finite displacements at the abutments on the structural behavior is considered in the works of Franciosi [4] and Ochsendorf [5].

The comprehension of the response of the masonry arch to environmental actions, as the earthquake or the yielding of abutments, must be completed. The previous work doesn't take into account the effects of horizontal loads and abutments finite displacements on the minimum thickness, for circular and pointed masonry arches.

In this paper the behavior of masonry arches at collapse is studied. In the first part the circular and pointed arch is considered to be supported by rigid abutments and the minimum thickness in the presence of both vertical and horizontal loads is determined. In the second part the condition of elastic abutments for the circular arch is analyzed; moreover, the influence of the flexibility of the piers on the minimum thickness is evaluated by a numerical procedure in large displacements.

# 2 RIGID ABUTMENTS

## 2.1 Geometrical description

The analysis is performed as a plane problem. The geometric characterization depends on the type of the considered masonry arch. Referring to the circular arch, the geometry is described by assigning the span *l*, the rise *f* and the thickness *s*, as shown in Figure 1(a). It follows that the central angle $\alpha$ subtended by the arch is uniquely defined.

Pointed arch needs an additional parameter; actually, the structure is determined by assigning the span *l*, the rise *f*, the thickness *s* and the angle θ (Figure 1(b)).

Let us denote by *d* the out of plane depth.

The analysis, both for the circular and the pointed arch, is carried out by the division of the structure into *n* voussoirs, which are numbered from left to right. The resulting *n+1* joints are obtained by radial cuts. The geometrical description of the structure, referring to a system of Cartesian axes *(z, y)*, requires the knowledge of *z* and *y* coordinates of the following points: center of gravity *G* of each voussoir, intrados *I* and extrados *S* of the radial joints, geometric centers *P* of the radial joints. The loading system consists of vertical and lateral pointed loads, which represent respectively the self-weight $F$ of each voussoir and the corresponding seismic action $F_s$. The latter is proportional to the vertical load through a multiplier $k$. Indeed it results:

$$F = \gamma_m \cdot A \cdot d \tag{1}$$

$$F_s = k \cdot F \tag{2}$$

where $\gamma_m$ represents the masonry's specific weight and $A$ the area of each voussoir. Without loss of generality it is assumed that the seismic action, i.e. the force $F_s$, is directed from left to right. See [6] for further detail regarding the parametric description of the arches.

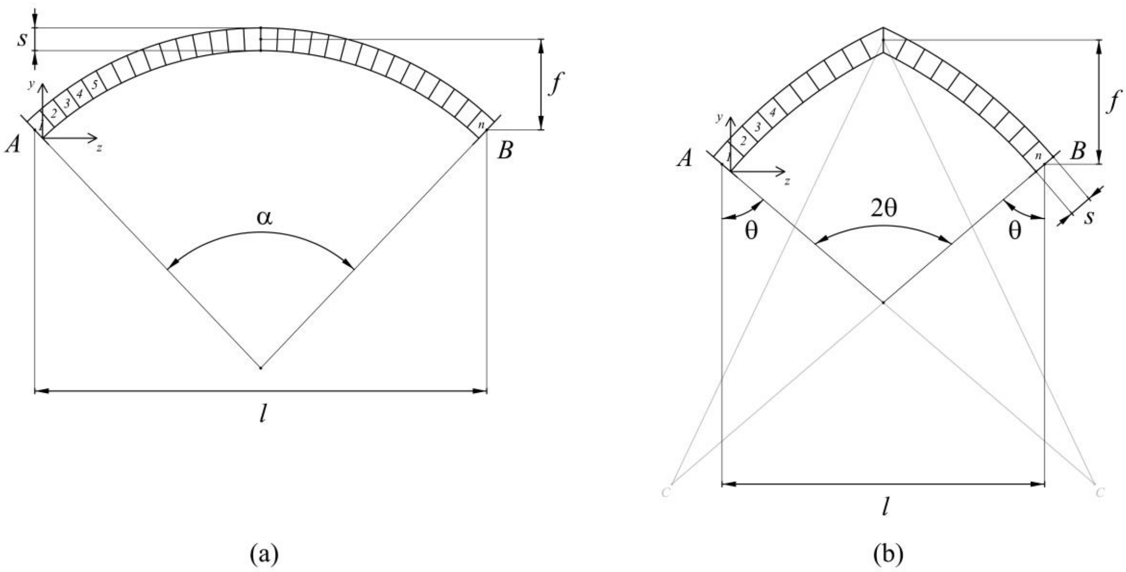


Figure 1: Geometry of circular (a) and pointed (b) masonry arch.

## 2.2 Balance conditions and numerical procedure

The purely rotational failure mechanism of an arch corresponds, in the presence of both vertical and horizontal loads, to a four-hinge mechanism [4] (Figure 2). It follows that at the collapse the arch is a statically determined structure, which can be solved by using balance conditions. Due to the non-symmetric nature of the problem, the position of the hinges can't be immediately defined.

Therefore, let us assume a first attempt configuration of hinges and impose the equilibrium in this collapse condition. From the static theorem of limit analysis, this equilibrated configuration results correct only if the corresponding line of thrust lies inside the masonry and passes through the assigned four hinges, namely if the resistance criterion for masonry is satisfied. If on the contrary the line of thrust falls outside the arch, the position of the hinges must be changed and the equilibrium imposed again; the solution can be attained by an iterative procedure. As suggested in [4], the best practical choice is to move the hinges where the distance between the center line of the arch and the line of thrust is maximum. So a few steps are required to get the right configuration.

Let us denote by *M*, *Q*, *T*, *U* the four collapse hinges corresponding to the *m*, *q*, *t*, *u* joints and by $V_U$, $H_U$ the vertical and horizontal reaction at hinge *U*; by taking the momentum balance about the remaining hinges one obtains:

$$\begin{cases} H_U(y_T - y_U) + V_U(z_T - z_U) - \sum_{j=1}^{n_{TU}} F_j(z_T - z_{G_j}) - k \cdot \sum_{j=1}^{n_{TU}} F_j(y_T - y_{G_j}) = 0 \\ H_U(y_Q - y_U) + V_U(z_Q - z_U) - \sum_{j=1}^{n_{QU}} F_j(z_Q - z_{G_j}) - k \cdot \sum_{j=1}^{n_{QU}} F_j(y_Q - y_{G_j}) = 0 \\ H_U(y_M - y_U) + V_U(z_M - z_U) - \sum_{j=1}^{n_{MU}} F_j(z_M - z_{G_j}) - k \cdot \sum_{j=1}^{n_{MU}} F_j(y_M - y_{G_j}) = 0 \end{cases} \tag{3}$$

where $n_{TU}$, $n_{QU}$, $n_{MU}$ refer respectively to the number of voussoirs between the joints *t*, *q*, *m* and *u*. The expression (3) is a determined system of equations, which can be solved in order to provide the reactions at hinge *U* and the load multiplier *k*.

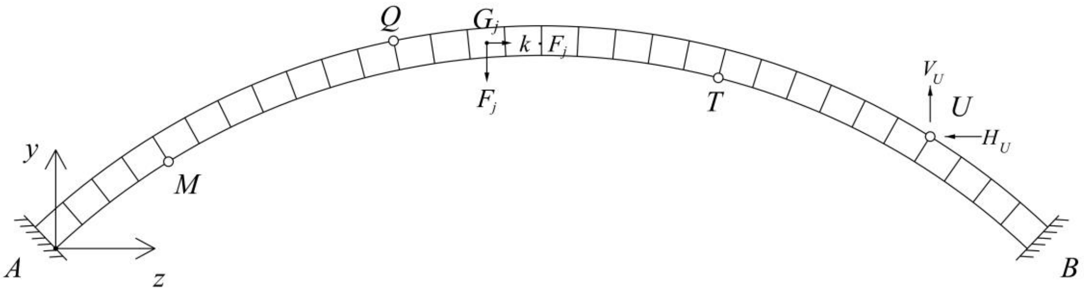


Figure 2: Generic four-hinge position associated to the collapse condition in the presence of vertical and horizontal loads.

The drawing of the line of thrust needs that the coordinates of the centers of pressure are known in correspondence of each radial joint, namely it requires the knowledge of the eccentricity of the normal force. Hence, by using expressions depending on the position of the joint, the resultant vertical and horizontal forces are defined (Figure 3(a)):

$$\begin{cases} H_i = H_U \mp k \cdot \sum_{j=1}^{n_{iu}} F_j \\ V_i = -V_U \pm \sum_{j=1}^{n_{iu}} F_j \\ M_i = V_U(z_U - z_{P_i}) + H_U(y_U - y_{P_i}) \mp \sum_{j=1}^{n_{iu}} F_j(z_{G_j} - z_{P_i}) \mp k \cdot \sum_{j=1}^{n_{iu}} F_j(y_{G_j} - y_{P_i}) \end{cases} \tag{4}$$

In the Equation (4), if the *i*th joint is at the left of hinge *U*, one has to use the upper sign, otherwise the lower one.

Thus, the normal force is known at each joint; by using respectively the upper and lower sign for the case $z_{Pi} < z_{Ii}$ and $z_{Pi} \geq z_{Ii}$:

$$N_i = H_i \cos\eta_i \pm V_i \sin\eta_i \tag{5}$$

where $\eta_i$ represents the angle between the line perpendicular to the *i*th joint and the horizontal one.

Finally, the eccentricity of the normal force is given by:

$$e_i = \frac{M_i}{N_i} \tag{6}$$

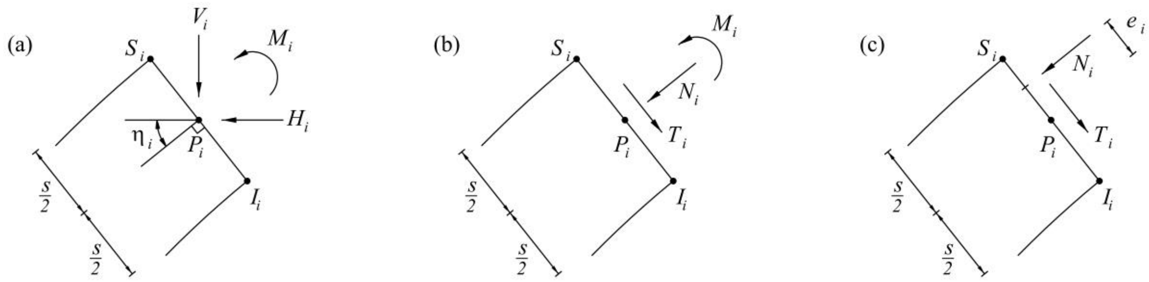


Figure 3: Stress state of the *i*th joint.

In order to check if the line of thrust, obtained by linking the centers of pressure, is anywhere inside the masonry, the following condition must be verified at each joint:

$$-\frac{s}{2} \le e_i \le \frac{s}{2} \tag{7}$$

It should be noticed that the sign of equality holds only in correspondence of the hinges *M*, *Q*, *T* and *U*.

As mentioned above, if Equation (7) is satisfied, then the position of hinges identifies the actual failure mechanism and the corresponding load multiplier. Otherwise, necessarily the hinges have to be moved in order to ensure that the static theorem is verified at each joint.

## 2.3 Results for circular arches

In order to point out the influence of geometry on the collapse of masonry arches, the relationship between the load multiplier *k*, the open angle $\alpha$ and the dimensionless thickness *s/l* is shown in Figure 4. Each curve was obtained by setting a constant value of the angle $\alpha$, progressively increasing the parameter *s/l* and evaluating the corresponding value of the collapse multiplier *k*. Notice that for the same thickness, the multiplier *k* increases with the decreasing of the angle $\alpha$. This means that the more the arch is lowered, the greater will be the resistance to horizontal actions, i.e. the earthquake.

In [1] Heyman studied the effects of geometrical properties on the stability of circular masonry arches subjected just to self-weight. He found the mathematical expression and the graphic trend of the minimum thickness that the arch should have to stand. In this work the study is extended by considering the presence of seismic action too, which is quantified through the load multiplier *k*. Figure 5 depicts graphically the minimum thickness for the circular masonry arch in the presence of an assigned seismic multiplier. The relationship is expressed between the half angle of embrace $\alpha/2$ and the dimensionless thickness *s/r*, being *r* the radius. By setting a constant value of *k*, namely by considering the individual curve, it results that the minimum thickness increases with the increasing of the angle of embrace.

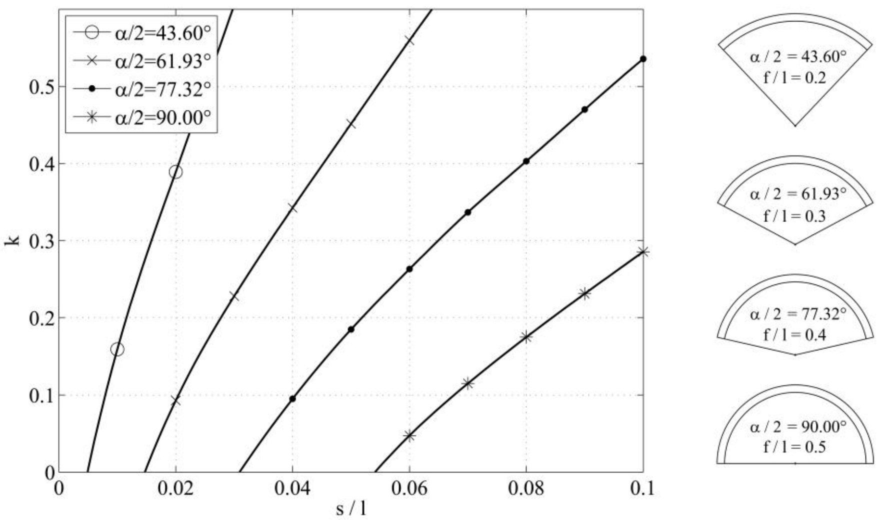


Figure 4: Load multiplier *k* of circular arches as function of geometry.

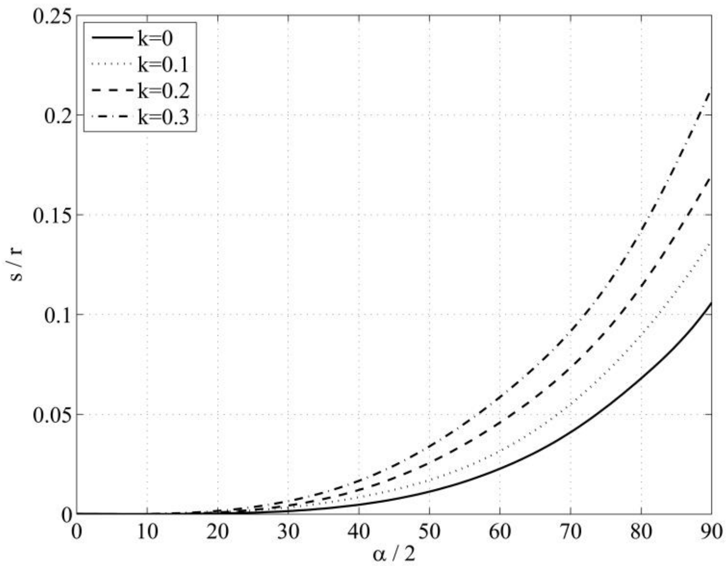


Figure 5: Minimum thickness for circular masonry arches with vertical and horizontal loads.

Geometrical features affects also the collapse horizontal thrust. In Figure 6(a) and 6(b) the path of the abutments horizontal thrust is shown. Each curve, relating to an assigned open angle $\alpha$, presents an upper and a lower branch, which intersect in a point corresponding to the Heyman's minimum thrust. This state corresponds, as known, to the arch subjected only to self-weight. The lower branch refers to the left abutment's thrust, while the upper branch identifies the right one. As expected, due to the previous assumption about the direction of horizontal loads, the path decreases in the first case and increases in the latter. In Figure 6 we denote by *W* the self-weight of the arch.

## 2.4 Results for pointed arches

The same procedure of analysis is extended to pointed arches. The effects of geometry are shown by comparing the circular arch, which has span $l$ and rise $f_0$, with pointed arches having the same span and different values of $f$ and $\theta$. We are considering two types of pointed arch, which differ from the ratio $f / f_0$.

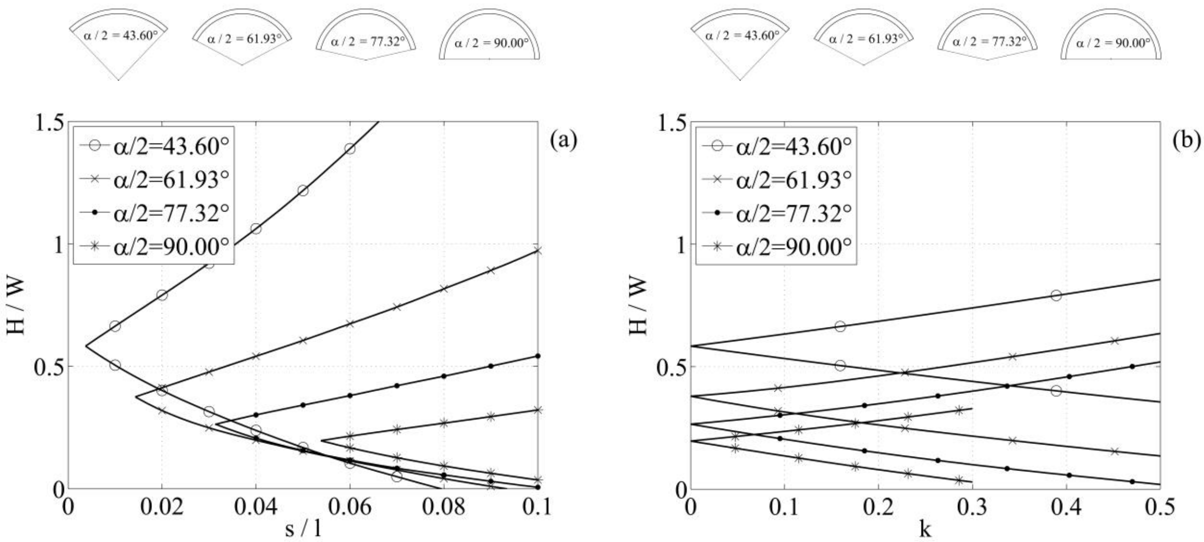


Figure 6: Normalized horizontal thrust for circular arches as function of the open angle $\alpha$ and of dimensionless thickness *s/l* (a), the angle $\alpha$ and of load multiplier *k* (b) (lower branch = left abutment thrust, upper branch = right abutment thrust).

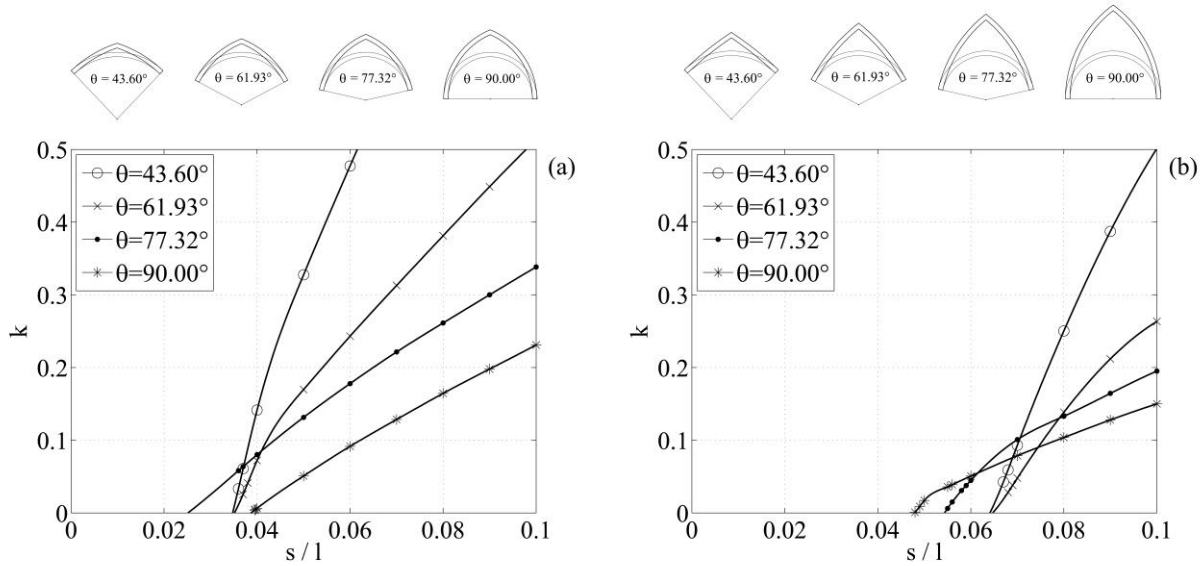


Figure 7: Load multipliers for pointed arches $f / f_0$ = 1.5 (a), $f / f_0$ = 2 (b).

Figure 7(a) refers to arches characterized by the ratio $f / f_0$ = 1.5, while Figure 7(b) corresponds to a value $f / f_0$ = 2. Each curve was determined by setting a constant value of the angle θ, progressively increasing the parameter *s/l* and evaluating the corresponding value of the collapse multiplier *k*. Notice that Figure 4 was obtained for a ratio $f / f_0$ = 1, i.e. for the circular arch.

Figure 8 corresponds to Figure 5, since it gives the minimum thickness for pointed masonry arches with $f / f_0$ = 1.5 (a) and $f / f_0$ = 2 (b) at different values of the load multiplier *k*, as function of the angle θ.

As shown above for circular arches, the graph of the abutment horizontal thrust is drawn in Figure 9 and 10; notice that the trend of the left and right thrust for pointed arches results similar to that of circular ones.

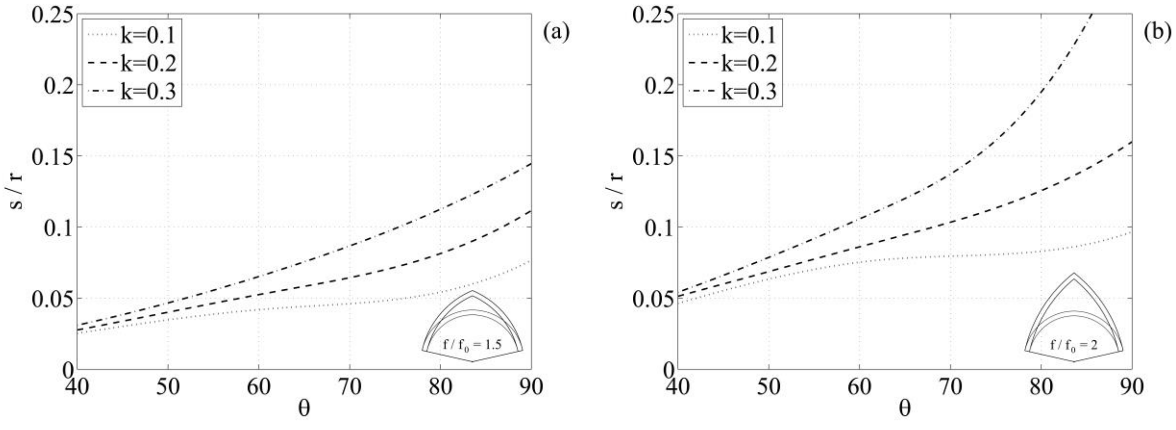


Figure 8: Minimum thickness for pointed masonry arches $f / f_0$ = 1.5 (a), $f / f_0$ = 2 (b).

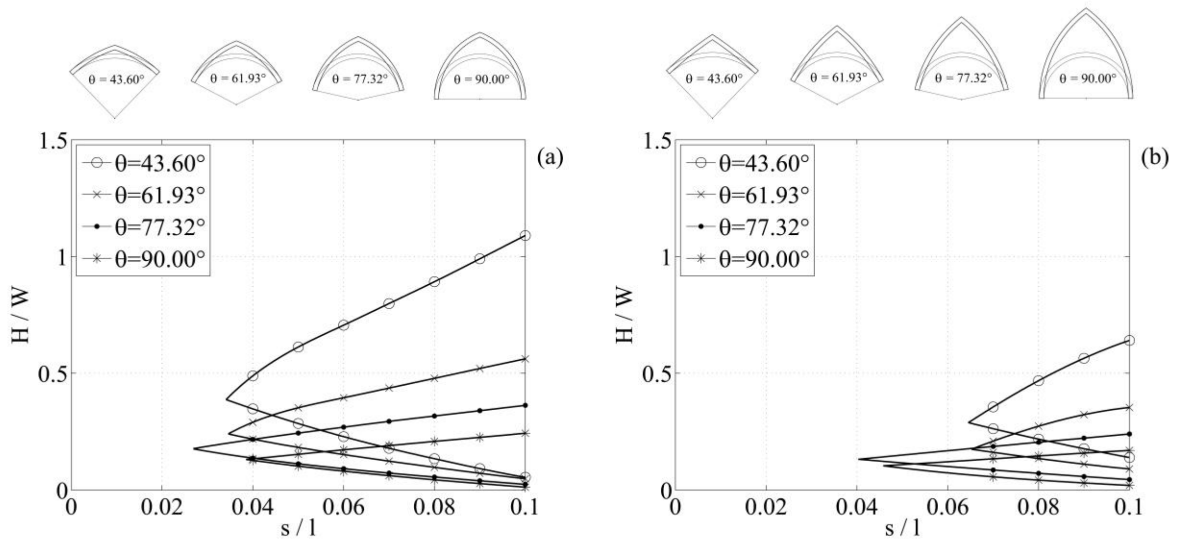


Figure 9: Normalized horizontal thrust for pointed arches $f / f_0$ = 1.5 (a), $f / f_0$ = 2 (b).

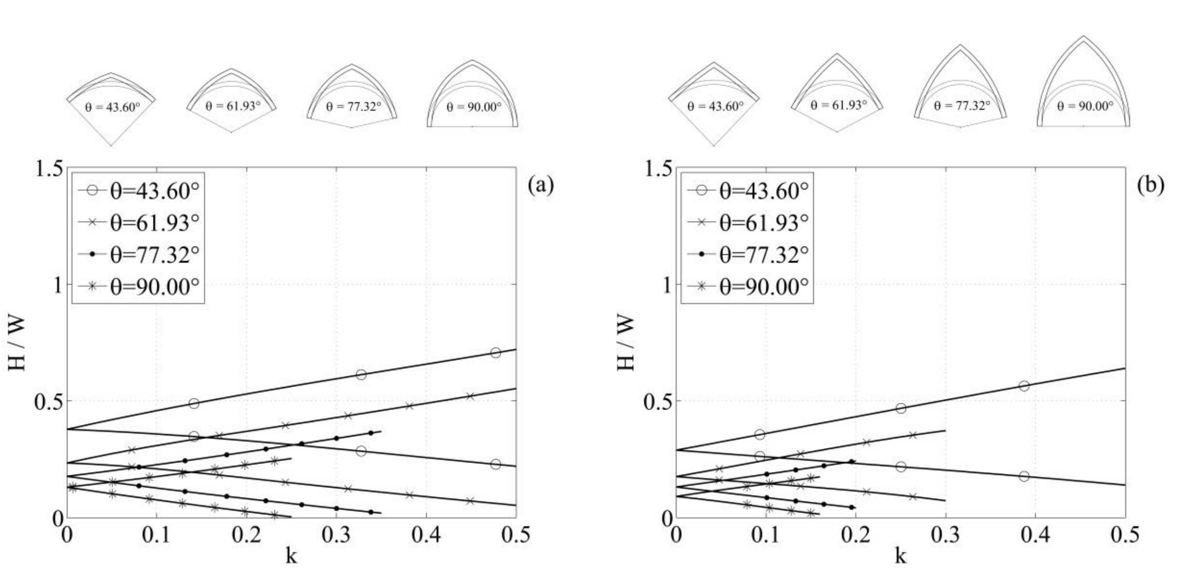


Figure 10: Normalized horizontal thrust for pointed arches $f / f_0$ = 1.5 (a), $f / f_0$ = 2 (b).

## 3 ELASTIC ABUTMENTS

If the abutments are perfectly rigid then the arch behaves as a rigid-plastic system, because an increasing horizontal load doesn't determine any displacement before the collapse. At failure, in correspondence to a four-hinge mechanism, undefined movements occur. On the contrary, if the structure has spreading supports, some hinges form at the beginning of the load history, when the self-weight starts acting after the removal of the rib: the arch is in the so-called minimum thrust condition. Heyman in [2] shows the shape of the line of thrust and indicates the arrangement of hinges.

Let us denote by δ the horizontal relative displacement of abutments, we assume:

$$\begin{cases} \delta = 0 & for\ k = 0 \\ \delta \neq 0 & for\ k \neq 0 \end{cases} \tag{8}$$

Conditions (8) mean that the abutments start spreading when horizontal loads are applied; instead, when it results $k$=0 the condition of little displacements is assumed. A non-zero horizontal load causes finite displacements of abutments and then the shift of static hinges, which correspond to the minimum thrust condition. The multiplier $k$ can increase until a limit value, corresponding to the collapse of the structure by the growing of a four-hinge mechanism.

The research of the collapse mechanism is carried out in accordance with the static theorem of limit analysis, by gradually increasing the horizontal displacement: the hinges arrangement corresponding to an equilibrated line of thrust that lies inside the masonry, is found at several values of δ. When this is no longer possible, it means that the failure condition is reached.

### 3.1 Kinematic description in finite displacements

The geometrical description of arches with rigid abutments, referred to in §2.1, is valid also for arches with elastic abutments in the minimum thrust condition.

The relationship between horizontal displacements $\delta_i$ and corresponding abutment reactions $R_i$ (with $i$=$A$, $B$) is assumed to be elastic and it's given by:

$$\begin{cases} c_A \cdot R_A = \delta_A \\ c_B \cdot R_B = \delta_B \end{cases} \tag{9}$$

with $\delta = -\delta_A + \delta_B$ and having denoted by $c_A$ and $c_B$ the two flexibilities at abutments.

For finite displacements, the kinematic description is made by referring to the Cartesian axes ($z'$, $y'$) having origin in the lower point of the first joint and modeling the arch as a system of two rigid links $TH$ and $HK$, both hinged at its ends (Figure 11(a)). The knowledge of $z'$ and $y'$ coordinates of the points of interest in the kinematic configuration ($G$, $I$, $P$ and $C$, referred to in §2.1) is needed in order to impose the equilibrium condition in large displacements.

### 3.2 Balance conditions and numerical procedure

By referring to the rigid links $TH$ and $HK$, six balance conditions can be written, including four translational and two rotational. In order to obtain a determined system, it is needed to add a further compatibility equation, which involves horizontal displacements at abutments. So one obtains:

$$\begin{cases} V_T + V_H - \sum_{j=1}^{n_{TH}} F_j = 0 \\ H_T + H_H + k \cdot \sum_{j=1}^{n_{TH}} F_j = 0 \\ V_T \cdot w_1 - H_T \cdot w_2 - \sum_{j=1}^{n_{TH}} F_j (z'_H - z'_{G_j}) - k \cdot \sum_{j=1}^{n_{TH}} F_j (y'_H - y'_{G_j}) = 0 \\ -V_H + V_K - \sum_{j=1}^{n_{HK}} F_j = 0 \\ -H_H + H_K + k \cdot \sum_{j=1}^{n_{HK}} F_j = 0 \\ -V_H \cdot w_3 + H_H \cdot w_4 - \sum_{j=1}^{n_{HK}} F_j (z'_K - z'_{G_j}) - k \cdot \sum_{j=1}^{n_{HK}} F_j (y'_K - y'_{G_j}) = 0 \\ -c_A (H_A - H_{Ag}) + c_B (H_B - H_{Bg}) = \delta \end{cases} \tag{10}$$

where: $V_T$, $V_H$, $V_K$ and $H_T$, $H_H$, $H_K$ denote vertical and horizontal reactions in the presence of seismic action at hinges *T*, *H* and *K*, $H_A$ and $H_B$ are the horizontal reactions at abutments in the presence of seismic action, $H_{Ag}$ and $H_{Bg}$ are the horizontal reactions at abutments in the presence of the only self-weight, $n_{TH}$ and $n_{HK}$ refers respectively to the number of voussoirs between the hinges *T-H* and *H-K*, $w_1 = a_1 \cos\beta_{1,def}$, $w_2 = a_1 \sin\beta_{1,def}$, $w_3 = a_2 \cos\beta_{2,def}$, $w_4 = a_2 \sin\beta_{2,def}$, with respectively $a_i$ and $\beta_{i,def}$ ($i$ = 1, 2) the length of the *i*th rigid link and the angle between the link and the horizontal line in large displacements. The equation system (10) can be solved in order to give the seven unknowns $V_T$, $V_H$, $V_K$, $H_T$, $H_H$, $H_K$ and *k*.

Then, as done above for rigid abutments, the normal force and the moment acting at each joint are determined in order to evaluate the eccentricity and the center of pressure. Last, the satisfaction of Equation (7) is verified, namely it is checked that the line of thrust lies everywhere inside the boundary of the arch. At several increasing values of the displacement δ, the equilibrium condition for the three-hinged arch and the shape of the line of thrust are determined, until it is no longer possible to assure the respect of Equation (7) because another hinge forms and leads to collapse.

### 3.3 Results for circular arches

The flexibility of abutments affects the collapse multiplier. In order to underline this effect, each curve of Figure 4 is redrawn by considering three different values of flexibility. In Figure 12 one can observe, by setting $c_A = c_B = c$, a constant dimensionless thickness *s/l* and a constant angle of embrace $\alpha$, the decreasing of *k* with the increasing of flexibilities. As expected, this means that the arch with spreading supports is more vulnerable than the arch with rigid ones.

Figure 13 depicts graphically the minimum thickness for circular masonry arches in the presence of an assigned seismic multiplier and for assigned values of flexibility at abutments. The relationship is expressed, as done in Figure 5 for rigid abutments, between the half angle of embrace α/2 and the dimensionless thickness *s/r*.

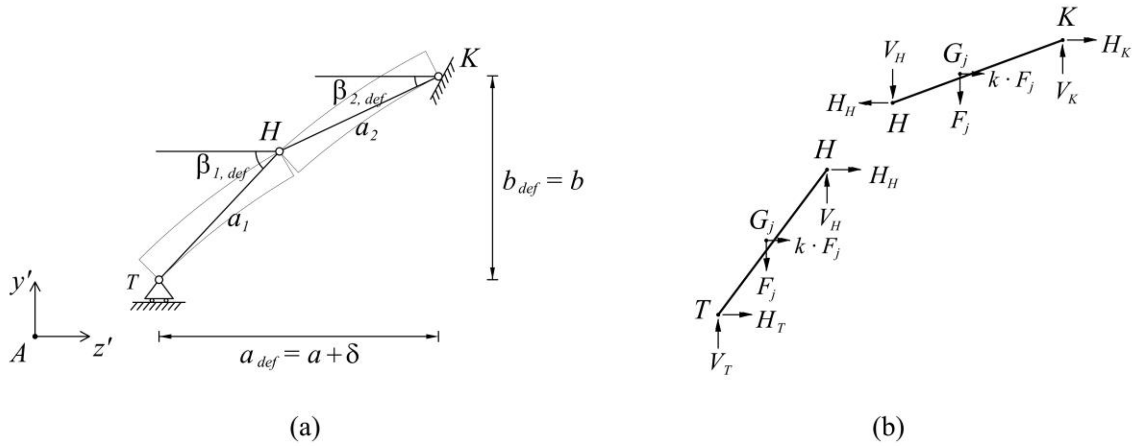


Figure 11: Kinematic description in large displacements (a) and forces acting on the two rigid links (b) - three hinged arch.

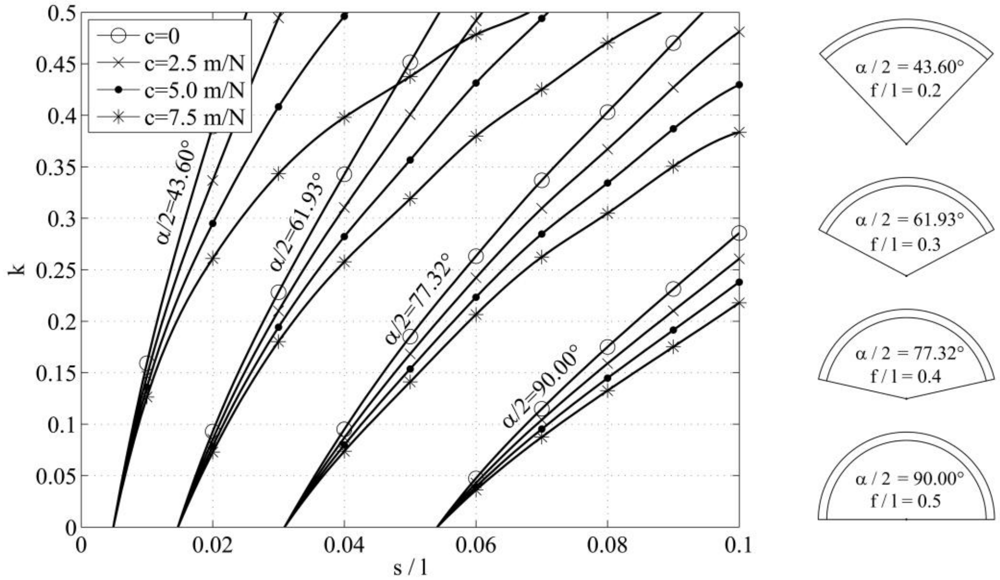


Figure 12: Load multipliers for circular arches as function of geometry and flexibility of abutments.

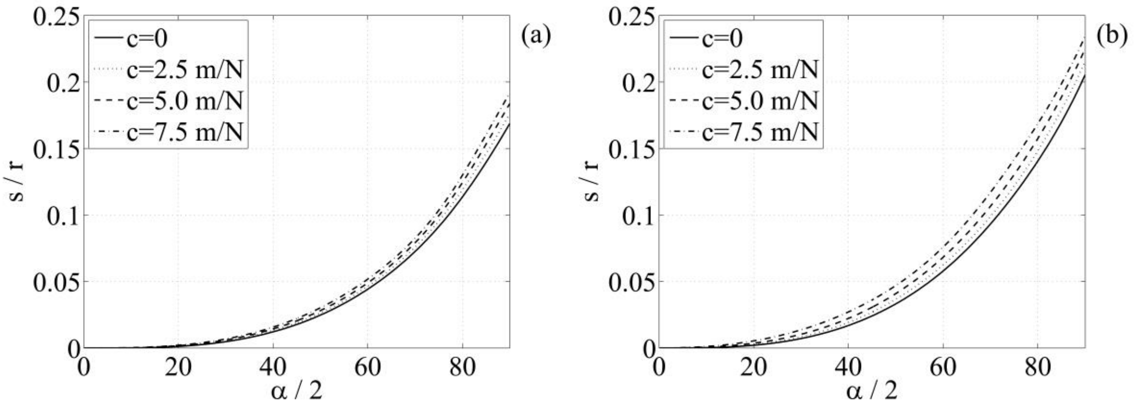


Figure 13: Minimum thickness for circular masonry arches with vertical and horizontal loads, at several values of flexibility - case $k$ =0.2 (a), case $k$ =0.3 (b).

## 4 CONCLUSIONS

The method of limit analysis has been applied in order to study the collapse condition of circular and pointed masonry arches, in the presence of vertical and horizontal loads. The analysis has been carried out by referring to Heyman's hypothesis about the masonry and considering the influence of the flexibilities of the abutments.

As extension of Heyman's results in the state of rigid abutments, the minimum thickness has been determined as function of the horizontal load multiplier and geometric features: it results an increasing minimum thickness with the increase of the horizontal load multiplier. The obtained curves could be a useful tool to define the thickness that the circular or the pointed arch should have to withstand an earthquake of assigned intensity.

Then, the minimum thickness analysis in the presence of both vertical and horizontal loads has been extended, for circular arches, to the condition of elastic abutments. The results have been obtained by imposing the equilibrium in large displacements. As could be expected, the analysis has shown that it is needed an increasing minimum thickness with the increase of the flexibility at the abutments and the obtained curves describe this relationship.

## REFERENCES

[1] J. Heyman, The safety of masonry arches. *International Journal of Mechanical Sciences*, **11**, 363-385, 1969.

[2] J. Heyman, *The masonry arch*. Ellis Horwood Ltd., Chinchester, 1982.

[3] A. Romano, J. Ochsendorf, The Mechanics of Gothic Masonry Arches. *International Journal of Architectural Heritage*, **4**(1), 59-82, 2010.

[4] C. Franciosi, Limit behavior of masonry arches in the presence of finite displacements. *International Journal of Mechanical Sciences*, **28**, 463-471, 1986.

[5] J. Ochsendorf, The Masonry Arch on Spreading Supports. *The Structural Engineer*, **84**(2), 29-36, 2006.

[6] L. Severini, *Analisi limite di archi in muratura in grandi spostamenti*, Master Thesis, University of Perugia, Italy, 2013 (in italian).